

# The host galaxy/AGN connection in nearby early-type galaxies <sup>\*</sup>.

## A new view of the origin of the radio-quiet/radio-loud dichotomy?

Alessandro Capetti<sup>1</sup> and Barbara Balmaverde<sup>2</sup>

<sup>1</sup> INAF - Osservatorio Astronomico di Torino, Strada Osservatorio 20, I-10025 Pino Torinese, Italy  
e-mail: capetti@to.astro.it

<sup>2</sup> Università di Torino, Via Giuria 1, I-10125, Torino, Italy  
e-mail: balmaverde@ph.unito.it

**Abstract.** This is the third in a series of three papers exploring the connection between the multiwavelength properties of AGN in nearby early-type galaxies and the characteristics of their hosts. Starting from an initial sample of 332 galaxies, we selected 116 AGN candidates requiring the detection of a radio source with a flux limit of  $\sim 1$  mJy, as measured from 5 GHz VLA observations. In Paper I we classified the objects with available archival HST images into “core” and “power-law” galaxies, discriminating on the basis of the nuclear slope of their brightness profiles. We used HST and Chandra data to isolate the nuclear emission of these galaxies in the optical and X-ray bands, thus enabling us (once combined with the radio data) to study the multiwavelength behaviour of their nuclei. The properties of the nuclei hosted by the 29 core galaxies were presented in Paper II. Core galaxies invariably host a radio-loud nucleus, with a median radio-loudness of  $\text{Log } R = 3.6$  and an X-ray based radio-loudness parameter of  $\text{Log } R_X = -1.3$ .

Here we discuss the properties of the nuclei of the 22 “power-law” galaxies. They show a substantial excess of optical and X-ray emission with respect to core galaxies at the same level of radio luminosity. Conversely, their radio-loudness parameters,  $\text{Log } R \sim 1.6$  and  $\text{Log } R_X \sim -3.3$ , are similar to those measured in Seyfert galaxies. Thus the radio-loudness of AGN hosted by early-type galaxies appears to be univocally related to the host’s brightness profile: radio-loud AGN are only hosted by core galaxies, while radio-quiet AGN are found only in power-law galaxies.

The brightness profile is determined by the galaxy’s evolution, through its merger history; our results suggest that the same process sets the AGN flavour. In this scenario, the black holes hosted by the merging galaxies rapidly sink toward the centre of the newly formed object, setting its nuclear configuration, described by e.g. the total mass, spin, mass ratio, or separation of the SMBHs. These parameters are most likely at the origin of the different levels of the AGN radio-loudness.

This connection might open a new path toward understanding the origin of the radio-loud/radio-quiet AGN dichotomy and provide us with a further tool for exploring the co-evolution of galaxies and supermassive black holes.

**Key words.** galaxies: active, galaxies: bulges, galaxies: nuclei, galaxies: elliptical and lenticular, cD, galaxies: nuclei, galaxies: structure

## 1. Introduction.

Despite the fundamental breakthroughs in our understanding of the nuclear regions of nearby galaxies, such as the ubiquitous presence of supermassive black holes (e.g. Kormendy & Richstone 1995), we still lack a clear picture of the relationship between AGN and host galaxies.

*Send offprint requests to:* A. Capetti

<sup>\*</sup> Based on observations obtained at the Space Telescope Science Institute, which is operated by the Association of Universities for Research in Astronomy, Incorporated, under NASA contract NAS 5-26555.

For example, while spiral galaxies preferentially harbour radio-quiet AGN, early-type galaxies host both radio-loud and radio-quiet AGN. Similarly, radio-loud AGN are generally associated with the most massive SMBH as there is a median shift between the radio-quiet and radio-loud distribution, but both distributions are broad and overlap considerably (e.g. Dunlop et al. 2003). Nonetheless, recent developments provide us with a new framework in which to explore the classical issue of the connection between host galaxies and AGN.

With this aim, we focused on two samples of nearby early-type galaxies for which extensive multiwavelength data from VLA, HST, and Chandra observations are available. This enabled us to study the multi-band behaviour of their nuclei in detail and, at the same time, to extract the structural parameters describing the host galaxies. More specifically we analysed the samples of early-type galaxies studied by Wrobel & Heeschen (1991) and Sadler et al. (1989), both observed with the VLA at 5 GHz with a flux limit of  $\sim 1$  mJy. Wrobel (1991) extracted a northern sample of galaxies from the CfA redshift survey (Huchra et al. 1983) satisfying the following criteria for a total of 216 galaxies: (1)  $\delta_{1950} \geq 0$ , (2) photometric magnitude  $B \leq 14$ ; (3) heliocentric velocity  $\leq 3000$  km s $^{-1}$ ; and (4) morphological Hubble type  $T \leq -1$ . Sadler et al. (1989) selected a similar southern sample of 116 E and S0 with  $-45 \leq \delta \leq -32$ . The only difference between the two samples is that Sadler et al. did not impose a distance limit. Nonetheless, the threshold in optical magnitude effectively limits the sample to a recession velocity of  $\sim 6000$  km s $^{-1}$ .

In Capetti & Balmaverde (2005, hereafter Paper I), we selected the 116 galaxies detected in these VLA surveys to boost the fraction of AGN with respect to a purely optically selected sample. We used archival HST observations, available for 65 objects, to study their surface brightness profiles and to separate these early-type galaxies following the Nukers scheme (Faber et al. 1997) rather than the traditional morphological classification (i.e. into E and S0 galaxies). Galaxies are then separated on the basis of the logarithmic slope  $\gamma$  of their nuclear brightness profiles in the two classes of “core” ( $\gamma \leq 0.3$ ) and “power-law” ( $\gamma \geq 0.5$ ) galaxies. For 51 galaxies the surface brightness profile is sufficiently well-behaved to yield a successful classification.

In the second paper, Balmaverde & Capetti (2006b, hereafter Paper II), we focused on the 29 “core” galaxies (hereafter CoreG). We found that core galaxies invariably host a radio-loud nucleus. Their radio-loudness parameters  $R$  is on average  $\text{Log } R = \text{Log} (L_{5\text{GHz}} / L_{\text{B}}) \sim 3.6$ . The X-ray data provide a completely independent view of their multiwavelength behaviour, leading to the same result, i.e. a large X-ray deficit, at the same radio luminosity, when compared to radio-quiet nuclei. Considering the multiwavelength nuclear diagnostic planes, the optical and X-ray nuclear luminosities are correlated with the radio-core power reminiscent of the behaviour of low luminosity radio-galaxies (LLRG). The inclusion of core galaxies indeed smoothly extends the correlations reported for LLRG (Balmaverde & Capetti 2006a) by a factor of  $\sim 1000$  toward lower luminosities, down to a radio luminosity of  $\nu L_{\nu} \sim 10^{36}$  erg s $^{-1}$ , covering a combined range of 6 orders of magnitude. A strong similarity between core-galaxies and classical low-luminosity radio-galaxies emerges, including the “core” classification, the presence of collimated radio-outflows, and the distribution of black-hole masses. Core galaxies and LLRG thus appear to be drawn from the same population of early-type galaxies; core-galaxies rep-

resent from the point of view of the level of nuclear activity a miniature version of the radio-galaxies.

Here we discuss the properties of the sub-sample formed by the 19 power-law galaxies (hereafter PlawG) and of the 3 galaxies with an intermediate nuclear slope, i.e. with  $0.3 < \gamma < 0.5$ .

We have adopted a Hubble constant  $H_0 = 75$  km s $^{-1}$  Mpc $^{-1}$ .

## 2. Basic data and nuclear luminosities

The basic data for the power-law galaxies, namely the recession velocity (corrected for Local Group infall onto Virgo), the K band magnitude from the Two Micron All Sky Survey (2MASS), the galactic extinction, and the total and core radio fluxes were given in Paper I. In the following three subsections, we derive and discuss the measurements for the nuclear sources in the optical, X-ray, and radio bands.

### 2.1. Optical nuclei.

Following the strategy outlined in Paper II for establishing whether an optical nuclear source is present at the centre of the objects of our sample, we relied on analysing the derivative of the surface brightness profile. In particular we looked for the characteristic up-turn that unresolved nuclear sources cause in the nuclear brightness profile, as opposed to the smooth decrease of the slope toward the centre when only a diffuse galactic component is present. Thus, we evaluated the derivative of the brightness profile in a log-log representation, combining the brightness measured over two adjacent points on each side of the radius of interest, yielding a second-order accuracy. We then looked for the presence of a nuclear up-turn in the derivative requiring a difference larger than  $3\sigma$  from the slopes at the local minimum and maximum for a nuclear detection.

This is a rather conservative definition, since i) the region over which the up-turn is detected extends over several pixels, while we only consider the peak-to-peak difference, and ii) a nuclear source can still be present but its intensity might not be sufficient to compensate for the downward trend of the derivative sets by the host galaxy, leading only to a plateau in the derivative.

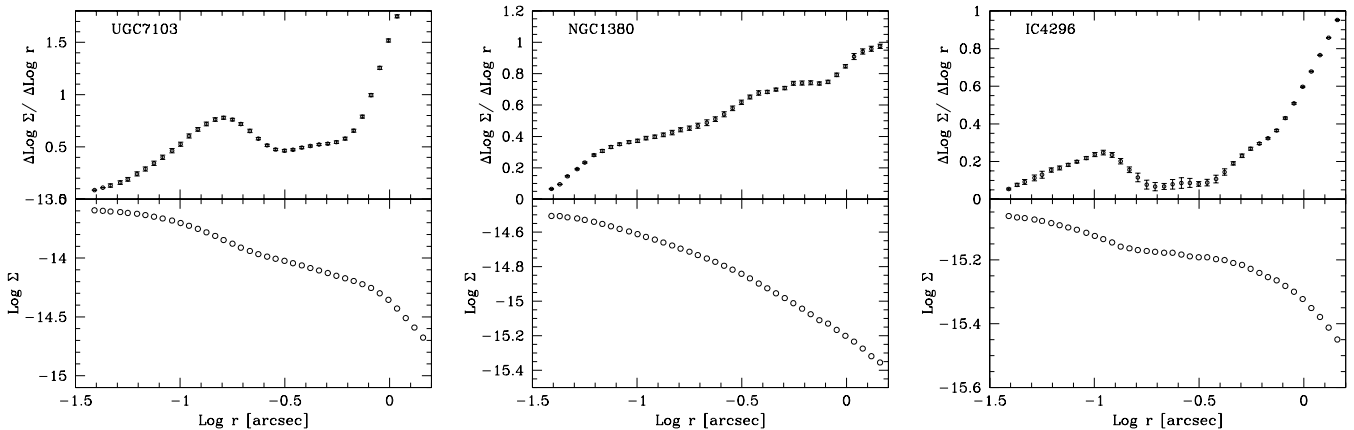
In Fig. 1 we report three examples. The brightness profile of UGC 7103 (left panel) clearly shows the presence of a nuclear source, with a highly significant increase in the derivative at about  $r = 0''.3$ . In NGC 1380 (middle panel) no up-turn in the brightness profile is seen, it is so considered as a non detection. The profile of the nucleated CoreG IC 4296 is shown as a comparison in the right panel.

In five cases, the optical images are strongly affected by the presence of dust absorption features. They not only prevent detailed study of their brightness profiles, but they also plague the measurements of the nuclear optical sources. For these objects we used the infrared HST images at  $1.6 \mu\text{m}$  to measure their nuclei. This approach appears to be reasonably justified within the context of

**Table 1.** Summary of the available Chandra and HST data.

| Name     | Chandra data summary |                |      | HST data summary |           |
|----------|----------------------|----------------|------|------------------|-----------|
|          | Obs. Id              | Exp. time [ks] | Ref. | Image            | $\nu F_0$ |
| UGC5617  | 860                  | 46.9           | (2)  | WFPC2/F702W      | <5.46E-13 |
| UGC5663  | 2926                 | 9.7            | (3)  | WFPC2/F702W      | 5.80E-13  |
| UGC5959  | –                    | –              | –    | WFPC2/F814W      | 5.74E-13  |
| UGC6153  | 2482                 | 89.4           | (4)  | NICMOS/F160W     | 2.73E-11  |
| UGC6860  | –                    | –              | –    | WFPC2/F814W      | <2.81E-13 |
| UGC6946  | –                    | –              | –    | WFPC2/F547M      | 3.10E-12  |
| UGC6985  | –                    | –              | –    | WFPC2/F814W      | <1.21E-12 |
| UGC7005  | –                    | –              | –    | WFPC2/F547M      | <1.64E-13 |
| UGC7103  | 1587                 | 15.0           | (1)  | NICMOS/F160W     | 1.27E-11  |
| UGC7142  | 1617                 | 2.8            | (5)  | WFPC2/F606W      | 5.37E-13  |
| UGC7256  | 397                  | 1.8            | (6)  | WFPC2/F814W      | 1.06E-12  |
| UGC7311  | –                    | –              | –    | WFPC2/F702W      | –         |
| UGC7575  | 2883                 | 25.4           | (7)  | WFPC2/F814W      | –         |
| UGC7614  | 2927                 | 9.9            | (1)  | WFPC2/F814W      | <7.61E-13 |
| UGC8355  | –                    | –              | –    | WFPC2/F702W      | 6.90E-13  |
| UGC8499  | –                    | –              | –    | WFPC2/F702W      | <1.00E-13 |
| UGC8675  | 415                  | 1.8            | (1)  | NICMOS/F160W     | 2.26E-12  |
| UGC9692  | –                    | –              | –    | WFPC2/F814W      | <5.26E-13 |
| UGC10656 | –                    | –              | –    | WFPC2/F702W      | <3.16E-13 |
| UGC12759 | –                    | –              | –    | NICMOS/F160W     | 1.81E-12  |
| NGC1380  | –                    | –              | –    | NICMOS/F160W     | <6.23E-13 |
| NGC6958  | –                    | –              | –    | WFPC2/F814W      | 1.90E-12  |

(1) this work, (2) George et al. (2001), (3) Filho et al. (2004), (4) Netzer et al. (2002), (5) Terashima &amp; Wilson (2003), (6) Ho &amp; Peng (2001), (7) Machacek et al. (2004).

**Fig. 1.** Brightness profile and its derivative for two PlawG: UGC 7103 (left panel) clearly shows the presence of a nuclear source, with a highly significant increase in the derivative at about  $r = 0''.3$ . In NGC 1380 (middle panel) no up-turn in the brightness profile is seen and it is considered as a non detection. The profile of the nucleated CoreG IC 4296 is shown as a comparison in the right panel. All 3 profiles presented are derived from the same filter/instrument combination (NICMOS/F160W) HST images.

a multiwavelength study spanning more than seven orders of magnitude in frequency, where the difference in frequency between optical and IR data is only marginal. We also note that the fraction of nuclei measured from IR data is rather small in both sub-samples of early type galaxies ( $\sim 24\%$ ).

Nonetheless, the use of IR measurements as a substitute for the optical nuclear fluxes is a potential cause of

concern<sup>1</sup>. First of all, this is related to the lower resolution of the NICMOS images, since at  $1.6 \mu\text{m}$  the diffraction limit of HST is  $\sim 0''.17$ , a factor  $\sim 2$  larger than in the optical images. Consequently, the detection threshold of an IR nucleus is higher than in the optical band. However, only one PlawG (and only one CoreG in Paper II) is undetected in the IR images, indicating that this is

<sup>1</sup> In Paper I we discussed a similar issue, showing that the Nuker classification is independent of the observing band.

not a significant issue. Similarly, the contrast against the galaxy's background might vary from the optical to the IR. However, the ratio between the optical (e.g. I band) and H band for the host galaxies, in terms of  $\nu F_\nu$ , is  $\sim 0.9$  for early type galaxies (Mannucci et al. 2001). Even adopting a wide range of values for the nuclear spectral index, e.g.  $\alpha \sim 0 - 2$ , the contrast between AGN and galaxy in the optical and IR images would differ by less than a factor of 2 (in either direction) in the two bands.

We also investigated the potentially worrying issue of how the fluxes of the 5 PlawG nuclei measured in the IR appear to be on average higher than those obtained from the optical images. In 2 cases, the optical nucleus has a luminosity (although measured with relatively large uncertainties due to the presence of dust) within 30 % of the IR nucleus. Three of them instead have X-ray data, and their X-ray nuclei are among the brightest in the sample, similar to what is seen for the IR data. This indicates that their nuclei are indeed brighter than average, regardless of the observing band used to measure their fluxes, and that this is not a bias introduced by the use of the NICMOS images. This effect is probably due to the connection between the presence of dust structures and nuclear activity (e.g. Lauer et al. 2005), since we used IR data for the dustier galaxies that are more likely to host bright AGN.

Adopting the strategy described above, we identified a nuclear source in the HST images in 11 out of 22 objects, four of them from IR data. We measured the nuclear fluxes (reported in Table 1) as in Paper II, i.e. integrating in a circular aperture with radius set at the location of the up-turn and as background region a circumnuclear annulus,  $0.1''$  in width. In 9 objects we did not find a nuclear upturn in the brightness profile, so they are considered as non detections. For the undetected nuclei we set as upper limits the light excess with respect to the starlight background within a circular aperture  $0.1''$  in diameter. In the remaining 2 objects (UGC 7311 and UGC 7575) the central regions are hidden by a kpc scale dust structure (see Fig. 2 in Paper I) so no measurement can be performed.

We derived all the luminosities referring to  $8140 \text{ \AA}$  (see Table 2) and adopting a spectral index<sup>2</sup>  $\alpha_o = 1$ .

## 2.2. X-ray nuclei.

For the measurements of the X-ray nuclei we concentrated on the Chandra measurements, as this telescope provides the best combination of sensibility and resolution necessary to detect the faint nuclei expected in these weakly active galaxies. Data for 9 power-law galaxies are available in the Chandra public archive. In Table 1 we give a summary of the available Chandra data, while references and details for the X-ray observations and analysis are presented in Appendix A.

When possible, we used the results of the analysis of the X-ray data from the literature. These are avail-

<sup>2</sup> We define the spectral index  $\alpha$  with the spectrum in the form  $F_\nu \propto \nu^{-\alpha}$

able for 6 sources, and in all cases they show the presence of a nuclear source, whose luminosity we rescaled to our adopted distance and converted to the 2-10 keV band, using the published power law index. We also considered the Chandra archival data for the 3 unpublished objects. We analysed these observations using the same strategy as in Balmaverde & Capetti (2006b). For 2 objects (namely UGC 4111 and UGC 8675) we obtained a detection of a nuclear power-law source. The data for one object (UGC 7614) do not lead to the detection of a X-ray nucleus. Details of the results are given in Appendix A, while the X-ray luminosities for all objects are given in Table 2.

## 2.3. Radio nuclei.

The radio data of our sample are drawn from the surveys by Wrobel & Heeschen (1991) and Sadler et al. (1989). Since they were obtained at a resolution of  $\sim 5''$ , they do not usually have a resolution sufficient, in the case of PlawG, to separate the core emission from any extended structure. Therefore, it is possible that these VLA data might overestimate the core flux.

We thus searched the literature for radio-core measurements obtained at a higher resolution (and/or higher frequency) than the VLA-survey data so as to improve the estimate of the core flux density. Better measurements from VLBI data or from higher frequency/resolution VLA data are available for most PlawG (17 out of 22)<sup>3</sup>.

These observations detected in 11 out of the 17 objects with available data. In Fig. 2 we compare the radio core flux density used in our analysis with the observations made at higher resolution. Overall there is substantial agreement between the two datasets. Considering only the detections, the median ratio between the high and low resolution data is  $\sim 0.80$ , with only one object whose offset is as large as a factor 3. Five of the upper limits are located close to the line of equal fluxes, while one of the undetected objects (UGC 5663) has a deficit larger than a factor of 6. Since these data are highly inhomogeneous and incomplete, and given the general agreement with the 5 GHz VLA measurements, we prefer to retain Wrobel's and Sadler's values. Nonetheless, in the rest of our analysis we always checked whether our results would be significantly affected using these higher resolution core fluxes.

## 3. The multiwavelength properties of the nuclei of power-law galaxies.

Having collected the multiwavelength information for the nuclei of our galaxies, we can now compare the emission in

<sup>3</sup> More specifically the radio-core fluxes are taken from Nagar et al. (2000) (15 GHz VLA data at  $0''.2$  resolution), Nagar et al. (1999) (8.4 GHz VLA data at  $0''.3$ ), Nagar et al. (2002) (15 GHz VLA data and 5 GHz VLBI data), Krajnović & Jaffe (2002) (8.4 GHz at the VLA), Filho et al. (2002) (VLBI data at 5 GHz), Filho et al. (2004) (VLA data at 8.4 and 5 GHz), and Slee et al. (1994) (PTI 8.4 GHz data).

**Table 2.** Power-law galaxies data.

| Name     | Log $L_X$ | Log $\nu L_o$ | Log $\nu L_{core}$ | Log $L_{[OIII]}$ | $M_K$  | Log ( $M_{BH}/M_\odot$ ) |
|----------|-----------|---------------|--------------------|------------------|--------|--------------------------|
| UGC5617  | 40.3      | < 40.51       | 36.88              | 38.75            | -22.80 | 8.07                     |
| UGC5663  | 38.8      | 40.57         | 36.87              | 38.59            | -23.58 | 8.32 <sup>b</sup>        |
| UGC5959  | –         | 40.54         | 37.16              | 38.95            | -23.73 | 8.43                     |
| UGC6153  | 42.4      | 42.11         | 38.14              | 40.79            | -24.43 | 7.42                     |
| UGC6860  | –         | <40.15        | 36.38              | 38.28            | -23.98 | 7.89                     |
| UGC6946  | –         | 41.40         | 38.16              | 39.42            | -23.80 | 8.87                     |
| UGC6985  | –         | <40.56        | 36.31              | –                | -23.39 | 7.93                     |
| UGC7005  | –         | <40.37        | 36.94              | 39.08            | -24.20 | 8.03                     |
| UGC7103  | 39.4      | 40.85         | 36.39              | 38.45            | -23.08 | 7.60                     |
| UGC7142  | 39.9      | 40.44         | 36.96              | 38.71            | -23.05 | 8.25                     |
| UGC7256  | 40.2      | 40.57         | 37.33              | 39.01            | -23.73 | 7.76                     |
| UGC7311  | –         | –             | 37.07              | –                | -23.76 | 8.30                     |
| UGC7575  | 39.3      | –             | 36.00              | 37.71            | -23.07 | 7.71                     |
| UGC7614  | <40.4     | <40.47        | 36.15              | <37.85           | -24.03 | 7.84 <sup>b</sup>        |
| UGC8355  | –         | 41.27         | 36.69              | –                | -22.75 | –                        |
| UGC8499  | –         | <40.37        | 37.09              | –                | -23.95 | 8.09                     |
| UGC8675  | 40.6      | 40.33         | 36.34              | 39.66            | -22.56 | 6.19                     |
| UGC9692  | –         | <40.41        | 36.65              | 37.78            | -23.85 | 8.63                     |
| UGC10656 | –         | <40.96        | 37.05              | –                | -24.00 | 7.63                     |
| UGC12759 | –         | 40.49         | 36.93              | 39.51            | -23.39 | 6.61                     |
| NGC1380  | –         | <39.96        | 36.68              | –                | -24.80 | 8.30                     |
| NGC6958  | –         | 41.46         | 38.10              | –                | -24.27 | 8.00                     |

Columns description: (1) UGC name, (2) nuclear X-ray luminosity (2-10 keV)[erg s<sup>-1</sup>], (3) nuclear optical luminosity (8140 Å) [erg s<sup>-1</sup>] corrected for absorption using the galactic extinction values in Paper I, (4) nuclear radio luminosity (5 GHz) [erg s<sup>-1</sup>] derived from Paper I, (5) [O III] line luminosity [erg s<sup>-1</sup>] from Ho et al. (1997), (6) total K band galaxy’s absolute magnitude from 2MASS, (7) logarithm of black hole mass in solar unity from <sup>b</sup> Marconi et al. (2003) or derived using the velocity dispersion.

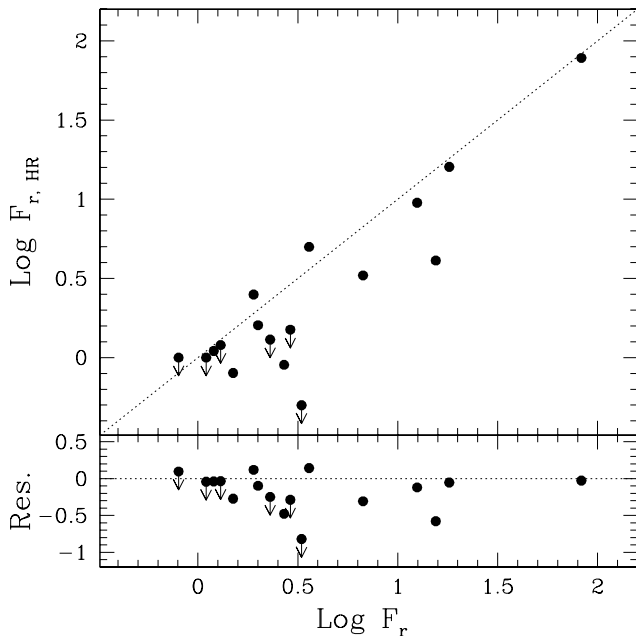


**Fig. 2.** Radio-core flux density for PlawG obtained at 5 GHz with the VLA (used in this work) compared to higher resolution data. See text for the references. The dotted line corresponds to equality.

the different bands. We detected an X-ray nuclear source in 8 out of 9 PlawG with available data, with only the exception of UGC 7614. Their representative points in the nuclear diagnostic diagram in which radio and X-ray luminosity are compared (see Fig. 3) are located well above the correlation defined by the CoreG and the LLRG. The upward offsets are between 0.8 and 3.3 dex, with a median of 1.8 dex.

A radio-loudness parameter based on the comparison between radio and X-ray luminosity (defined as the ratio of the radio-luminosity at 5 GHz and the 2-10 keV X-ray luminosity, i.e.  $R_X = \nu L_r / L_X$ ) has been recently introduced by Terashima & Wilson (2003). For PlawG we find values in the range  $\text{Log } R_X \sim -3 - -4.3$ <sup>4</sup> with a median value of  $\text{Log } R_X \sim -3.3$ . These values are very similar to those obtained by Terashima & Wilson (2003) for the nuclei of Seyfert galaxies, and indeed 3 PlawG are spectroscopically classified as Seyfert by Ho et al. (1997). Conversely the radio-to-X-ray luminosity ratios for PlawG are substantially lower than the median value obtained for the radio-loud nuclei of the core galaxies, for which we found  $\text{Log } R_X \sim -1.3$ .

Overall, the optical observations confirm this picture. The 11 galaxies with a detected optical nucleus are located

<sup>4</sup> The only exception is UGC 5663 with  $\text{Log } R_X = -1.9$ . However, this object is not detected in the VLBI observations discussed in Sect. 2. This indicates that a value of  $\text{Log } R_X \lesssim -2.7$  is probably a more accurate estimate.

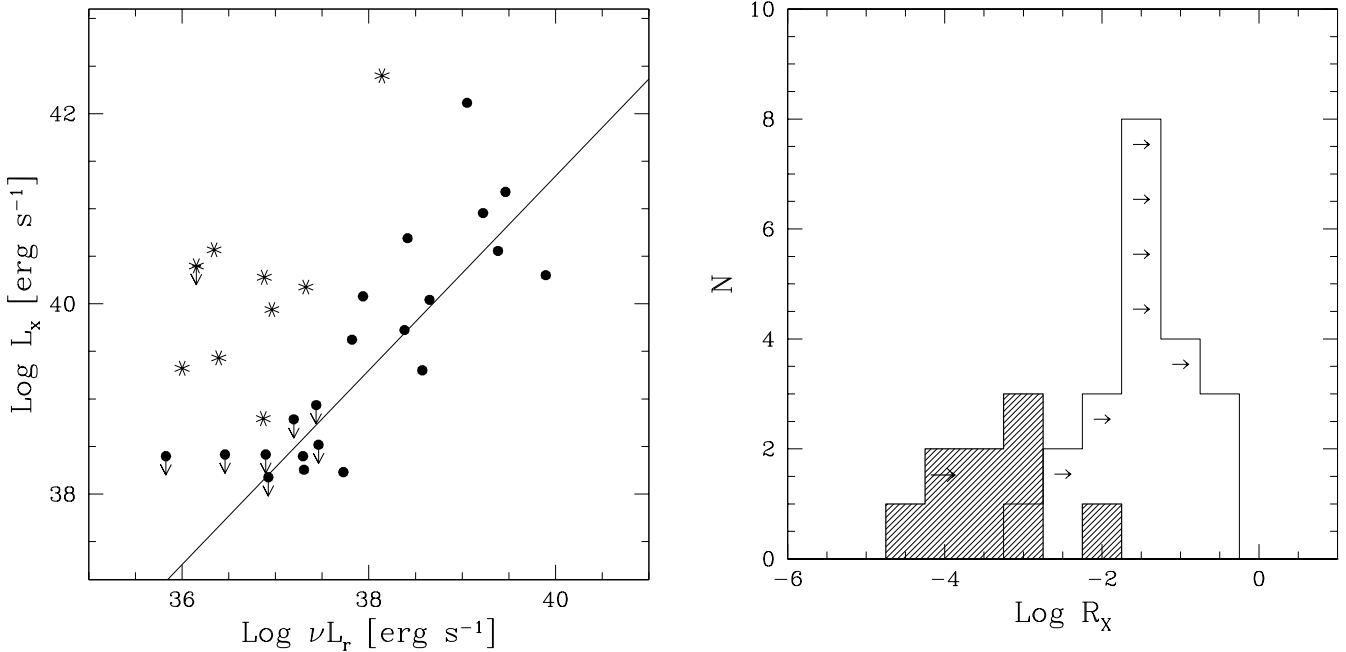


**Fig. 3.** Left panel: comparison of radio and X-ray nuclear luminosity for the sample of power-law galaxies (stars) and for the core galaxies (filled circles). The solid line represents the correlation derived in Paper II between the nuclear luminosities of the sample formed by CoreG and the 3C/FR I sample of low luminosity radio-galaxies. Right panel: radio-loudness parameter  $R_X$  estimated from the ratio of radio and X-ray nuclear luminosity, i.e.  $R_X = (\nu L_r / L_X)$ , for PlawG (filled histogram) and CoreG (empty histogram).

between 1.7 and 3 orders of magnitude above the  $L_r$  vs  $L_o$  correlation found for CoreG (see Fig. 3, left panel). All optical upper limits are located in the same region of the radio vs. optical plane of the detected nuclei. Nonetheless, the relatively large fraction of upper limits warrant a more detailed discussion of this issue, which will be presented in the next sub-section.

In Fig. 4, right panel, we compare the distributions of the standard radio-loudness parameter  $R = L_{5\text{GHz}} / L_B$  (Kellermann et al. 1994) having converted the optical luminosity to the B band with an optical spectral index of  $\alpha = 1$ . It shows the presence of an overall shift of about two orders of magnitude between the two classes of early-type galaxies.

Here the traditional separation into radio-loud and radio-quiet AGN ( $\text{Log } R = 1$ , e.g. Kellermann et al. 1994) is probably inappropriate since this is based on the observations of AGN with much higher luminosity, mostly bright QSOs. In fact the results presented by Ho & Peng (2001) clearly show that there is a strong evolution of the radio-loudness parameter with luminosity. This smoothly increases from a typical value of  $\text{log } R \sim -1$  for QSO with  $M_B \sim -24$  to  $\text{log } R \sim 0 - 2$  in Seyfert nuclei, the same range covered by PlawG.

We conclude that both radio-loudness parameters,  $R$  and  $R_X$ , for PlawG are a factor of  $\sim 100$  smaller than in the radio-loud nuclei of CoreG, while they are in close agreement with the values measured in radio-quiet AGN with a similar level of nuclear luminosity.

The comparison of the optical emission line luminosities provides another tool to explore the multiwavelength properties of PlawG and CoreG nuclei. In the compilation of Ho et al. (1997) we find measurements of the [O III] line for most of the objects forming the Northern sample (see Table 2). In Paper II we noted that CoreG extend the correlation between radio-core and line luminosity found for low luminosity radio-galaxies (Capetti et al. 2005). Conversely, PlawG have a line luminosity that is highly enhanced with respect to CoreG at the same level of radio-luminosity (see Fig. 5). This is a further indication that in PlawG the active nucleus provides (at a given  $L_r$ ) a substantially larger flux of ionizing photons with respect to CoreG, in line with the higher luminosity in the optical and X-ray bands.

It is also interesting that the equivalent widths of the [O III] emission line (Fig. 5, right panel), estimated against the HST optical nucleus, nicely fit the trend of EW with luminosity presented by (Dietrich et al. 2002), with the values measured for the PlawG again in the same range as those of Seyfert galaxies.

We finally note that in our sample there are 3 galaxies with a cusp slope that is intermediate between CoreG and PlawG,  $0.3 < \gamma < 0.5$ , namely UGC 7005, UGC 7575, and UGC 8675. Since they were not discussed in Paper II, where only CoreG were presented, we included them in the present analysis. In UGC 8675, we detected both an optical and a X-ray nucleus. The nuclear regions of UGC 7575 are obscured by a kpc dusty disk, but this object has

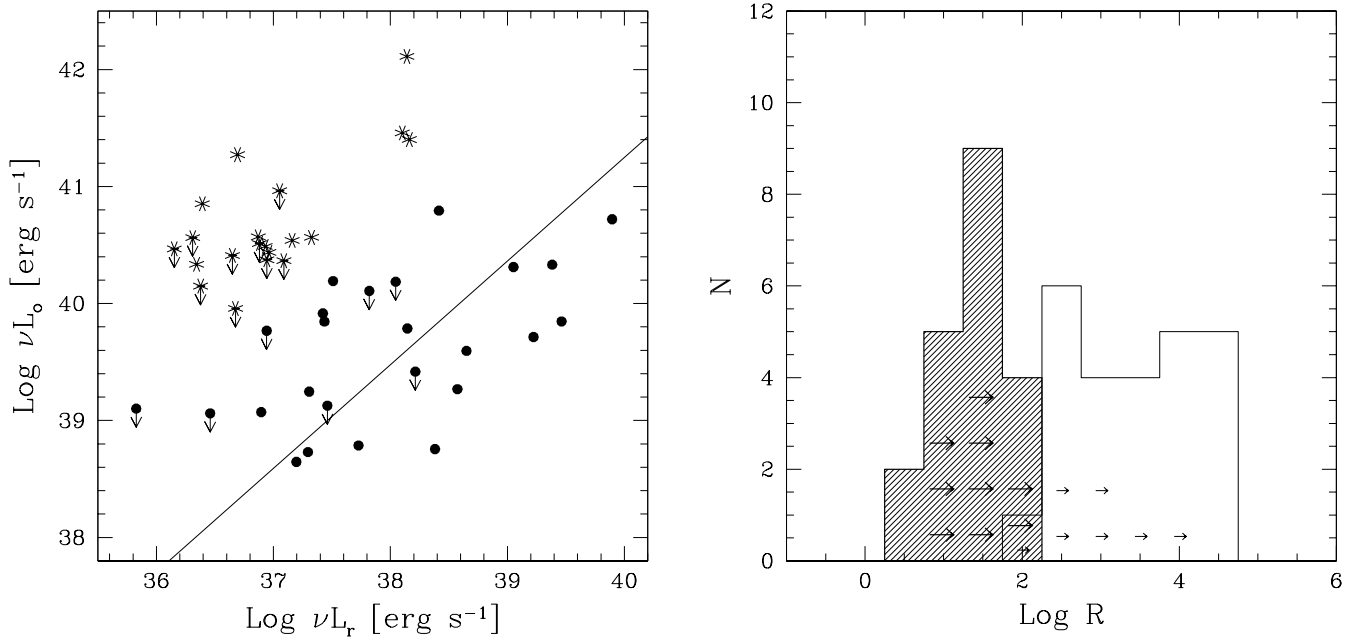


**Fig. 4.** Same as Fig. 3 but using the optical nuclear luminosity. Left panel: comparison of radio and optical luminosity for the PlawG (stars) and CoreG (filled circles). The solid line represents the correlations derived in Paper II between the nuclear luminosities of the sample formed by CoreG and the 3C/FR I sample of low luminosity radio-galaxies. Right panel: comparison of the radio-loudness parameter  $R = L_{5\text{GHz}} / L_B$  for PlawG (filled histogram) and CoreG (empty histogram); larger, heavier arrows mark the upper limits for PlawG, while smaller arrows are associated with CoreG upper limits.

a detected X-ray nucleus. Their radio-loudness parameters are close to the average for PlawG. The nucleus of UGC 7005 remains undetected in the HST images (and no X-ray data are available), but its radio and [O III] luminosities ( $L_r = 10^{36.94} \text{ erg s}^{-1}$  and  $L_{[\text{OIII}]} = 10^{39.08} \text{ erg s}^{-1}$ , respectively) locate this object within the region covered by PlawG. We conclude that the nuclear properties of these 3 intermediate galaxies (from the point of view of brightness profile) are indistinguishable from those of bona fide PlawG.

### 3.1. Undetected optical nuclei in power-law galaxies.

As noted above, an optical nucleus is not detected in several PlawG: in 2 cases the presence of large scale dust lanes prevent from exploring their optical nuclear properties altogether, while for 9 objects we were only able to set an upper limit. This substantial fraction is also related to our quite conservative definition of a nucleated source. Despite the overall agreement between upper limits and detections, this raises the possibility that faint nuclei, characteristic of CoreG, might be associated with these objects.

In fact, the minimum detection level for a nucleus in a PlawG is on average substantially higher than for the CoreG, due to the higher brightness in the nuclear regions

of PlawG<sup>5</sup> as well as to the steeper slope of the brightness profiles close to the centre. This is explained better by comparison of the results obtained for the analysis of the brightness profile of a CoreG (IC 4296) (Fig. 1, right panel) and for the two PlawG presented in this same figure. The flux of the clearly detected nucleus of the CoreG IC 4296 is a factor 7 smaller than the upper limit set for the PlawG NGC 1380.

This bias in the detection threshold due to the different optical brightness profiles might potentially affect the strength of the separation between the two classes in the diagnostic planes and in the distribution of radio-loudness parameters. However, we have various indications that this is not the case.

First of all, the X-ray observations are not affected by this bias and the detection rate here is  $\sim 90\%$ . The X-ray detections also lead to a radio-quiet classification for UGC 5617 and UGC 7575, two objects lacking the optical measurement. The non detection of an optical nucleus in the first galaxy, is most likely due to nuclear obscuration since this is a well-studied Seyfert type 2 (AKA NGC 3226). In UGC 7575 the optical obscuration is due to a kpc dusty disk that is clearly visible in the HST images. This result emphasizes that, not unexpectedly, the optical data can be plagued by the presence of absorption,

<sup>5</sup> The two classes have similar brightness at the break radius, see Fig. 10 in Paper I, but the PlawG have by definition steeper nuclear slopes, leading to higher nuclear brightness.

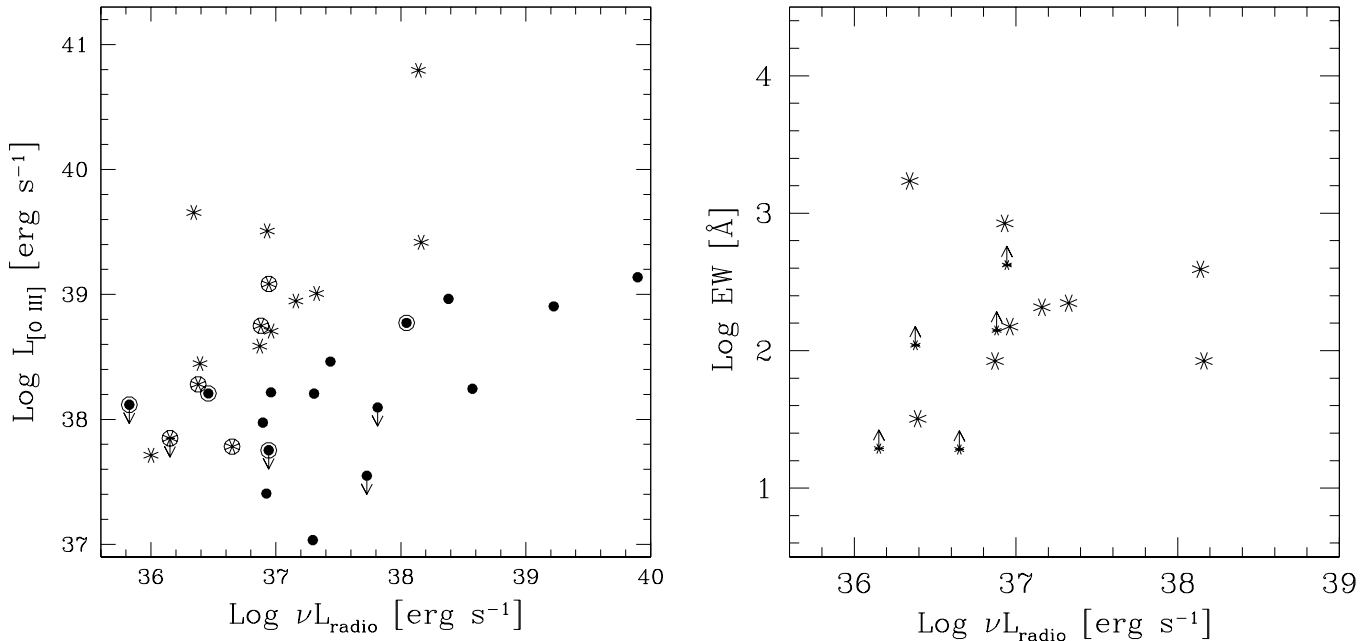


**Fig. 5.** Left) [O III] emission line vs. radio-core luminosity for PlawG (stars) and CoreG galaxies (filled circles). Symbols enclosed in a circle mark objects with undetected optical nuclei. Right) Equivalent width of the [O III] emission line with respect to the nuclear continuum luminosity.

accounting for some non detections. Considering the line vs. radio luminosity diagram now, we have line measurements for 5 of the undetected nuclei (indicated as stars within a circle in Fig. 5). Three of them are all located in the same region of the optically detected PlawG. This indicates that when supporting X-ray or spectral information are available, they suggest in general a classification as radio-quiet AGN, even for the objects in which the optical nucleus is undetected.

Finally, we must note that our sample can be contaminated by the presence of non active galaxies. In fact, we selected AGN candidates that only require a detection above  $\sim 1$  mJy in radio observations, but in some cases this might be produced by processes unrelated to an AGN. In Paper II we sought confirmation of a genuine AGN by looking for the presence of i) an optical (and X-ray) core, ii) an AGN-like optical spectrum, or iii) radio-jets. For the CoreG we are left with 3 (out of 29) unconfirmed AGNs. For the PlawG, 6 galaxies do not fulfill any of these criteria. Not surprisingly, they are all at the faint end of the radio-luminosity distribution. Among them, for example, there is UGC 7614, the only galaxy undetected in the X-ray, as well in the optical and in VLBI observations, with a low radio-luminosity ( $\text{Log } L_r = 36.15$ ) and with only a tentative spectral classification as a transition source between HII and LINER galaxies (Ho et al. 1997).

### 3.2. Power-law vs. core galaxies and radio-loud vs. radio-quiet hosts

The results presented above indicate that the multiwavelength properties of the nuclei of the PlawG differ significantly from those of CoreG, with an optical (and X-ray) excess of about 2 orders of magnitude at equal radio-luminosity, and that a similar separation is found comparing the emission line luminosities. We here explore in more detail how PlawG and CoreG also compare from the point of view of other parameters, such as the host’s luminosity, black-hole mass, and optical spectra. Given the association between brightness profile class and radio-loudness, this same line of reasoning can be used to test whether radio-loud and radio-quiet AGN differ on the basis of these parameters.

The PlawG are  $\sim 1$  magnitude fainter than CoreG, (see Fig. 6 left panel), with median values of  $M_K = -23.8$  and  $M_K = -24.8$  for PlawG and CoreG, respectively. This reflects the well-known result that the brightest early-type galaxies only show “core” profiles. However, the two classes coexist below  $M_K = -25$ .

To compare their black-hole masses, when no direct measurement (taken from the compilation by Marconi & Hunt 2003) was available, we estimated  $M_{BH}$  using the relationship with the stellar velocity dispersion (taken from the LEDA database) in the form given by Tremaine et al. (2002). The distributions of  $M_{BH}$  of the two samples are compared in Fig. 6. PlawG have a median value,  $\text{Log } M_{BH} = 8.0$ , which is about a factor of 3 lower than for CoreG,  $\text{Log } M_{BH} = 8.5$ . While no CoreG has



a black-hole mass smaller than  $\text{Log } M_{BH} = 7.6$ , among PlawG there are two outliers from the PlawG distribution, UGC 8675 and UGC 12759, with estimated masses of a few  $10^6$  solar masses. As already found for the host's luminosity, however, a large overlap between the black-hole masses is present.

Considering the optical spectra, among PlawG we have 3 objects classified as Seyfert and 11 as LINER. For the CoreG, we found 13 LINER and one galaxy with diagnostic line ratios that are on the borderline between LINER and Seyfert. This, on the one hand, confirms the result obtained by Chiaberge et al. (2005) that a dual population is associated with galaxies with a LINER spectrum, being formed by both radio-quiet and radio-loud objects. On the other the bulk of the two sub-samples of early-type galaxies are associated with similar low-ionization optical spectra, while possibly Seyfert nuclei are hosted only by PlawG. Therefore, no clear subdivision of early-type galaxies can be obtained relying on the host galaxies luminosity, black hole mass, or optical spectrum.

This result can be extended to a possible link of these parameters to the radio-loudness of AGN. This point is made clearer by Fig. 7, in which we plot the optical radio-loudness parameter against the black-hole mass and the host's luminosity. Although the most massive black holes are associated only with radio-loud nuclei, and the 2 least massive ones to radio-quiet AGN, both classes are found for the range  $8 \lesssim \text{Log } M_{BH} \lesssim 9$ . A possible distinction based on the galaxy's magnitude is even less clear, since it only emerges that galaxies brighter than  $M_K \lesssim -25$  exclusively host radio-loud AGN: below this level both classes of radio-loudness are found down to the luminosity limit of the sample, with the least luminous galaxy associated with a radio-loud nucleus.

Consequently, the only univocal connection linked to the different radio-loudness class of the AGN hosted by early-type galaxies is found when considering their brightness profiles. This is clearly shown by the right panel in Fig. 7, where we report radio-loudness against  $\gamma$ , the logarithmic slope of the brightness profile. This figure also shows that, when the two classes are separated, there is no dependence of  $R$  on the nuclear slope.

#### 4. Constraints on the accretion process.

Taking advantage of the estimates of black-hole mass we can refer the measurements of the nuclear luminosities to units of the Eddington luminosity. PlawG nuclei are associated with a fraction of  $L_{\text{Edd}}$  covering a large range,  $L/L_{\text{Edd}} \sim 10^{-3} - 10^{-7}$ , in both the X-ray and optical bands (see Fig. 8), extending down to the regime characteristic of advection dominated accretion flows (ADAF, Narayan & Yi 1995; Narayan 2004). When compared to the CoreG, PlawG correspond to higher values of  $L_{\text{Edd}}$ ; indeed, the two distributions match closely when a shift of about 2 orders of magnitude is applied. This reflects the difference in their nuclear luminosities, which is further enhanced by the slightly higher  $M_{BH}$  values for CoreG.

The differences between the properties of the two classes are even more prominent considering that in CoreG the correlations between radio, optical and X-ray luminosities strongly suggest that most likely we are seeing emission produced by an outflow. For this class the measured Eddington ratios should probably be considered as upper limits to any emission from the accretion disk. In PlawG the non-thermal jet radiation is likely to represent a negligible contribution to the light seen in the optical and X-ray. The observed nuclear light most likely represents the genuine radiative output of the accretion process.

For the CoreG with the least luminous X-ray nuclei, the analysis performed by Pellegrini (2005) shows that these can be explained only if an important role is played by outflows (or by convection) to substantially suppress the amount of gas actually reaching the central object. In fact, their extremely low luminosity levels appear to contrast even with the estimates of the fiducial minimum accretion rate derived for the case of spherical accretion.

The constraints for PlawG are clearly less stringent. This is firstly due to the substantially higher nuclear luminosities in Eddington units. Furthermore, the spherical accretion rate scales as  $\dot{M}_B \propto \rho T^{-3/2} M_{BH}^2 \propto \rho M_{BH}^{1.44}$  (having used  $T \propto \sigma^{1.5}$  as a proxy for the temperature and  $M_{BH} \propto \sigma^{4.02}$ ) where  $\rho$  and  $T$  are the density and temperature of the circumnuclear gas. Unfortunately, detailed studies of X-ray data, potentially leading to estimates of  $\rho$  and  $T$ , are not available for PlawG. However, unless the central densities are substantially enhanced in PlawG with respect to CoreG, the minimum accretion rate is expected to be lower for this first class of objects.

Therefore, it appears that only in CoreG is it necessary to advocate an outflow to reduce the accretion rate to a level compatible with the low nuclear luminosities. Interestingly, this is the same class for which the widespread detection of radio-jets indicates the presence of a highly collimated outflow. We speculate that a common mechanism might drive both phenomena of ejection.

#### 5. Discussion and conclusions

The aim of this series of three papers has been to explore the classical issue of the connection between host galaxies and AGN, in the new light shed by the recent developments in our understanding of the nuclear regions of nearby galaxies.

In Paper I we selected two samples of nearby galaxies comprising 332 early-type objects. We derived a classification into core and power-law galaxies, based on the nuclear slope of their optical brightness profiles measured from the available HST images. This has been possible for a sub-sample of 51 AGN candidates, selected by imposing the detection of a radio source at a flux limit of  $\sim 1$  mJy at 5 GHz.

In Paper II we focused on the 29 ‘‘core’’ galaxies. We used HST and Chandra archival data to isolate the nuclear emission of these galaxies in the optical and X-ray bands, thus enabling us (once combined with the radio

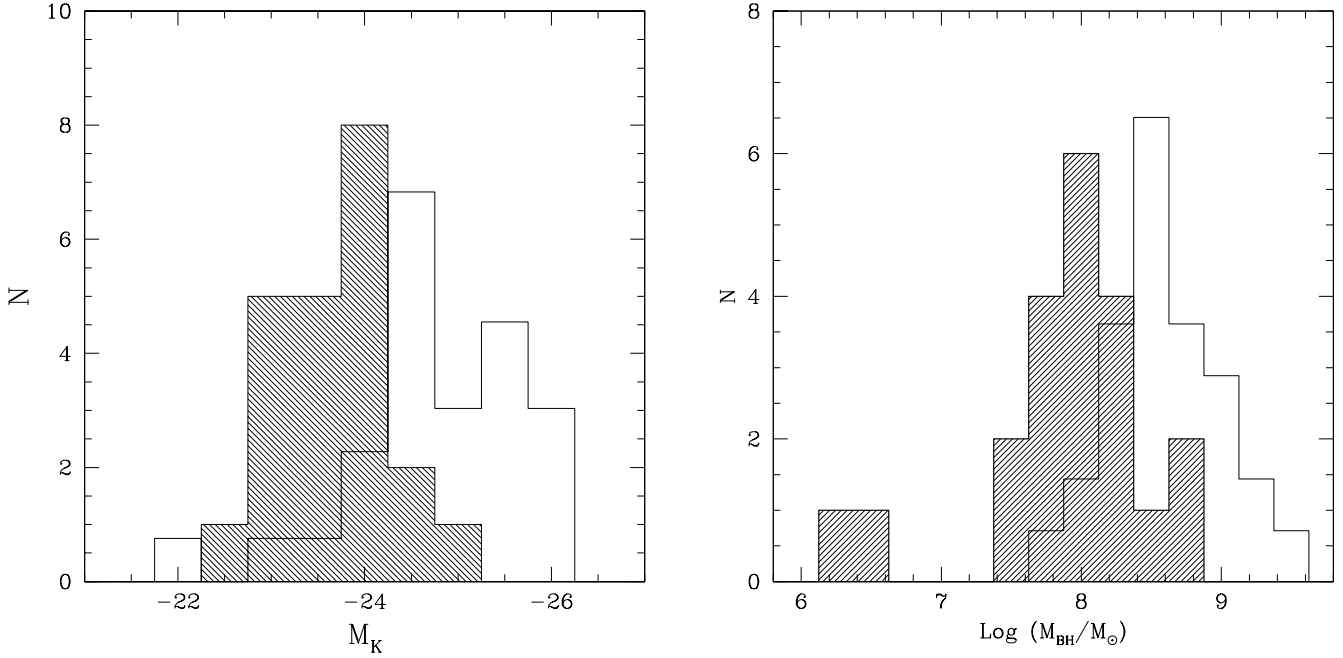


**Fig. 6.** Distributions for PlawG (shaded histograms) and for CoreG (empty histogram) of (left panel) absolute magnitude  $M_K$  and (right panel) black-hole mass  $M_{BH}$ . The CoreG histograms have been re-normalized multiplying by a factor 29/22 for  $M_{BH}$  and 29/21 for  $M_K$ , respectively, i.e. the number of objects in the two samples for which estimates of these parameters are available.

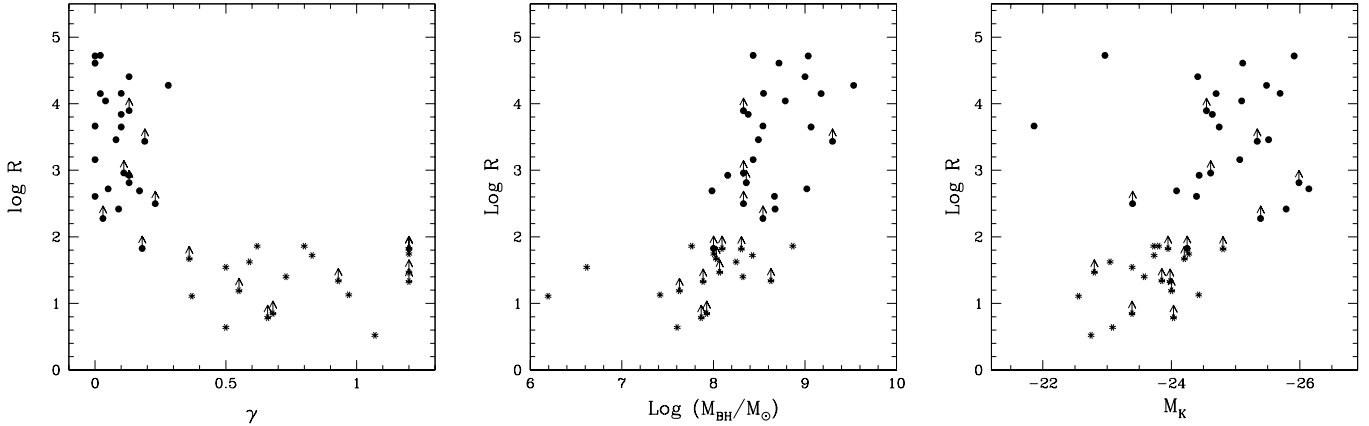


**Fig. 7.** Radio-loudness parameter  $R$  vs. (left) estimated black-hole mass and (centre) galaxies absolute magnitude. Stars represent power-law galaxies, circles mark core galaxies. No clear separation between radio-loud and radio-quiet nuclei can be obtained based on these two quantities alone. (Right) radio-loudness vs.  $\gamma$ , the logarithmic slope of the brightness profile. Power-law galaxies in which no break in the brightness profile is seen above the resolution limit are set arbitrarily to  $\gamma = 1.2$ .

data) to study the multiwavelength behaviour of their nuclei. We found that core galaxies invariably host a radio-loud nucleus, with an average radio-loudness of  $\text{Log } R = \sim 3.6$ . The X-ray data provide an independent view of their multiwavelength behaviour leading to the same result, with an X-ray-based radio-loudness parameter of  $\text{Log } R_X = \text{Log}(\nu L_r/L_X) \sim -1.3$ .

In this third paper, we report the analysis of the properties of power-law galaxies. PlawG show an excess of

about 2 orders of magnitude for their optical and X-ray nuclear luminosity with respect to the correlation defined by CoreG and LLRG at a given radio-core power. This translates into substantially lower radio-loudness parameters with median values of  $\text{Log } R \sim 1.6$  and  $\text{Log } R_X \sim -3.3$ . These values are similar to those measured in Seyfert galaxies.

Thus the radio-loudness of AGN hosted by early-type galaxies appears to be univocally related to the host's

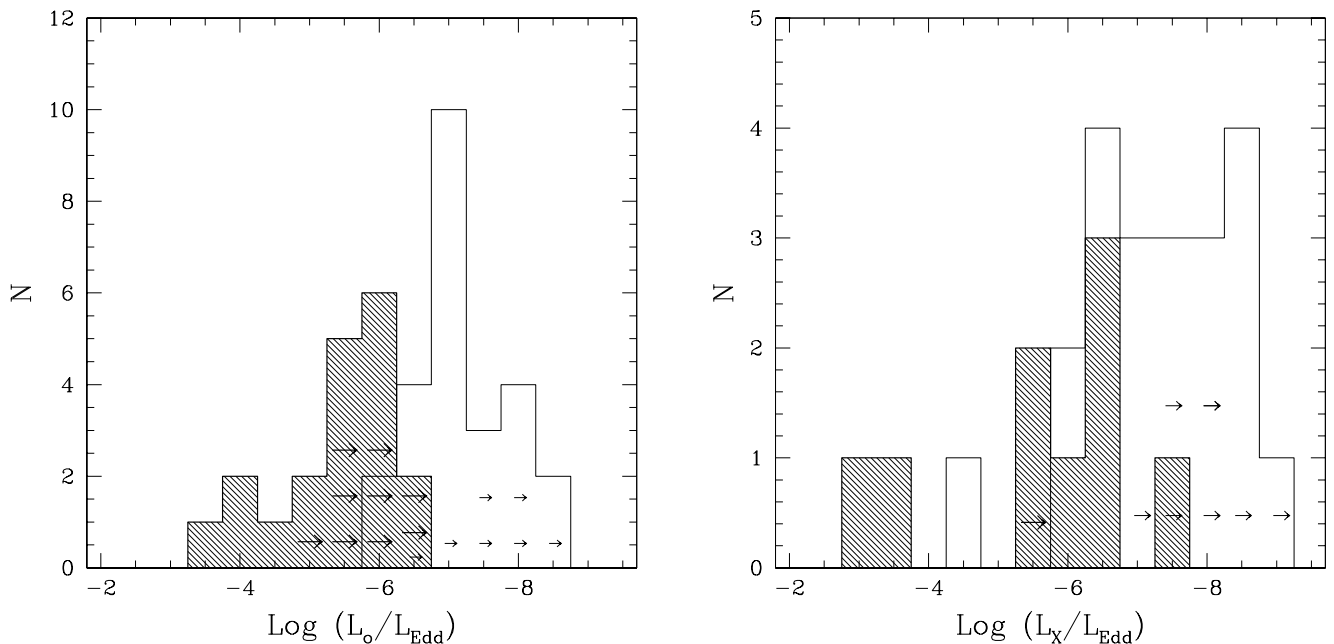


**Fig. 8.** Distributions of the nuclear luminosities measured as fractions of the Eddington luminosity in the optical (left) and the X-ray (right) bands for the PlawG (shaded histogram) and CoreG (empty histogram). Upper limits for PlawG are marked with larger and heavier arrows.

brightness profile: radio-loud AGN are only hosted by core galaxies while radio-quiet AGN are found only in power-law galaxies.

Radio-loud and radio-quiet nuclei in our sample cannot be distinguished on the basis of other parameters, such as the host’s luminosity, the black-hole mass (they differ only on a statistical basis), or the optical spectral classification. This reflects the situation, discussed in the Introduction, encountered in the past when trying to understand the connection between host galaxies and AGN. Only the brightness profiles provide a full separation between the two classes.

In the Introduction we also reported that spiral galaxies only harbour radio-quiet AGN (with the notable exception of the radio-source 0313-192, Ledlow et al. 1998). Seigar et al. (2002) shows that spiral galaxies in which the large scale spheroids can be described with a  $R^{1/4}$ -law (as opposed to exponential bulges) also show steep nuclear cusps in HST images, with  $\gamma > 0.5$ . This is indicative of a similarity between these luminous bulges and the early-type power-law galaxies. The  $R^{1/4}$ -law bulges are usually found in spiral galaxies of Hubble type  $T \lesssim 3$  that also represent the predominant host type for Seyfert galaxies (e.g. Maia et al. 2003). This fits nicely with our finding that radio-quiet nuclei are associated with galaxies with a power-law brightness profile and suggests an extension of this link also to spiral hosts.

A possible interpretation of the connection between the brightness profile and the AGN radio-loudness relies on the different formation processes of core and power-law galaxies. In fact, it has been suggested that a core

galaxy is the result of (at least) one major merger and that the core formation is related to the dynamical effects of the binary black holes on the stellar component (e.g. Milosavljević et al. 2002; Ravindranath et al. 2002). Conversely, power-law galaxies partly preserve their original disk appearance, suggestive of a series of minor gas-rich mergers (Faber et al. 1997; Ryden et al. 2001; Khochfar & Burkert 2003). The surface brightness profile thus results from the formation history of the galaxy, via mergers. The merger process also involves the SMBH associated with each galaxy that rapidly sink toward the centre of the forming object (Begelman et al. 1980). The connection between the properties of the galaxy (i.e. its mass and velocity dispersion) and the black-hole mass sets a link between the characteristics of the newly formed galaxy and the system of binary black holes at its centre. The resulting nuclear configuration after the merger (described by e.g. the total mass, spin, mass ratio, or separation of the SMBHs) is then directly related to the evolution of the host. These same parameters are most likely at the origin of the different levels of the AGN radio-loudness.

Several different aspects of the merger process must be explored to take full advantage of our result as to explore the origin of the radio-loud/radio-quiet dichotomy, as well as to provide a further tool for exploring the co-evolution of galaxies and supermassive black holes in this context. In particular, it is still unclear whether, and under which conditions, the black holes at the centre of the newly-formed galaxy coalesce (e.g. Makino & Funato 2004). This has a very important impact on the AGN physics. For example, among the different viable interpre-

tations, Wilson & Colbert (1995) suggested that a radio-loud source can form only after the coalescence of two SMBH of similar (large) mass, forming a highly spinning nuclear object, from which the energy necessary to launch a relativistic jet can be extracted. Note that, in this situation (the merging of two large galaxies of similar mass) the expected outcome is a massive core-galaxy, in line with our results.

Substantial progress in our understanding of the dichotomy of the brightness profiles is also required, mainly from the point of view of the relationship between the galaxies formation history and their brightness profiles. Detailed N-body simulations exploring a wide range of masses and mass-ratios between the merging galaxies, including the effects of the black holes, are still not available. But the situation is far from settled also from the point of view of modeling the observed brightness profiles. For example, the Nuker's fitting strategy has been challenged by Graham et al. (2003). They argue that a Sérsic model (Sérsic 1968) characterises the brightness profiles of early-type galaxies better. It is unclear whether the dichotomy in early-type galaxies found by Faber et al. (1997) is preserved when this different strategy is adopted. When our sample is concerned, the situation appears to be rather clear, since all objects we classified as core-galaxies are recovered as such according to the Graham et al. definition too. This is probably due to the fact that we are dealing with nearby galaxies, with well-resolved cores, and covering a rather limited range in absolute magnitude.

From our data we cannot establish whether the separation between radio-loud and radio-quiet objects and the relationship with the brightness profile is associated with a smooth transition or whether it is the manifestation of a threshold effect. From the point of view of the radio-loudness measurements, although PlawG and CoreG are well separated, there is no gap in their radio-loudness distributions. In part this is due to the scatter (in addition to the dispersion intrinsic of each class) introduced by measurement errors and by nuclear variability, since the multiwavelength data are not simultaneous. The relatively small number of objects with complete multiwavelength coverage and the presence of upper limits inhibits a detailed analysis of this issue. The lack of a dependence of  $R$  on the nuclear slope (once PlawG and CoreG are separated) argues against the existence of a continuity between the two classes of early-type galaxies. Furthermore, at least one of our selection criteria, i.e. the detection of a radio source, biases the sample toward the inclusion of the radio-quiet AGN with higher radio-loudness parameters. In this sense our sample of low-luminosity AGN is likely to represent only the tail, toward high values of  $R$ , for the overall population of radio-quiet AGN. If this is the case, the separation between the two classes might be even more pronounced. It is interesting that even for QSOs the issue of the distribution of radio-loudness parameters is still a matter for debate, in particular concerning the influence of the biases introduced by the methods of sample selec-

tion on the observed dichotomy (see e.g. Cirasuolo et al. 2003).

Our data were also used to explore the radiative manifestation of the accretion process onto the supermassive black holes hosted by early-type galaxies. CoreG have nuclear luminosities  $\sim 2$  orders of magnitude fainter than PlawG. This is somewhat surprising since there is evidence that in CoreG there is a substantial contribution from jet emission, which should make them brighter, everything else being equal, than PlawG. Since the least luminous PlawG are already in the regime characteristic of low efficiency accretion flows, e.g. ADAF, this difference is most likely due to a lower accretion rate in CoreG. We have speculated that a common mechanism might drive both the relativistic jets commonly observed in the radio-loud CoreG, as well as an outflow (originating at larger radii), which reduces the accretion rate to a level compatible with their low nuclear luminosities.

Our analysis is based on a sample of nearby galaxies (since only in galaxies at relatively small redshift is it possible to separate galaxies with different brightness profiles with high confidence) and this results in the selection of AGN of low luminosity. It would be very interesting to assess whether the association between AGN radio-loudness and host profile can be extended to more luminous AGN. In de Ruiter et al. (2005) we demonstrated that radio-galaxies (with both FR I and FR II morphology), on average far brighter than those found in our sample, are hosted exclusively by core galaxies, indicating that our scenario applies to radio-loud AGN with a radio-luminosity as large as  $L_r \sim 10^{42}$  erg  $s^{-1}$ . For the radio-quiet objects, the case of Seyfert galaxies is very promising. Not only is there a substantial population of nearby Seyfert galaxies hosted by early-type galaxies, but in the case of Type 2 galaxies the nucleus is obscured at optical wavelengths. This leaves open the possibility of exploring their nuclear brightness profiles in detail and to test the prediction that they should be hosted by power-law galaxies. Unfortunately this cannot be expected, at least in the near future, for quasars that combine larger distances and even brighter nuclei than Seyfert galaxies. However, a wider applicability of the connection between AGN properties and brightness profiles, might provide useful insights also for the interpretation of the results obtained from the study of QSO host galaxies.

The results presented here can be put on stronger ground with new observations. For example, the X-ray data provide us with the clearest separation between the two classes. This is due to the combination of two effects with respect to the optical data: 1) the X-ray data are not subject to the bias of detecting faint nuclei in galaxies with high optical brightness and 2) they are less affected by nuclear obscuration. Observing time with the Chandra telescope has been recently awarded to us to obtain full coverage with X-ray data of the Northern sub-sample.

Similarly, the available radio data are often not adequate for isolating and measuring the radio-cores accurately. For example, VLBI observations of the PlawG

UGC 5663 provided an upper limit of 0.5 mJy (Filho et al. 2004) to be compared with the 3.3 mJy VLA flux; its radio-loudness parameter, the larger among the radio-quiet nuclei, is then actually an upper limit. But, most important, the lack of high sensitivity radio observations completely inhibits the multiwavelength study of all galaxies undetected in the radio surveys. The detection of fainter radio-sources associated with early-type galaxies has the potential to expand the sample with complete multiwavelength coverage by a factor of 3 and, at the same time, to extend our study to an even lower level of radio power.

Substantial progress can also be expected from new HST data. First of all, they can lead to a Plawg/CoreG classification for a larger fraction of objects in the sample, currently only at a  $\sim 44\%$  level. Near-infrared HST observations are likely to provide useful brightness profiles in the significant fraction of objects whose optical structure is plagued by the presence of dust features. Finally, observations at shorter wavelength, where the contrast between the nuclear emission and the galactic starlight is enhanced, might allow the detection of a higher fraction of optical sources with respect to the available images.

*Acknowledgements.* This work was partly supported by the Italian MIUR under grant Cofin 2003/2003027534\_002. This research made use of the NASA/IPAC Extragalactic Database (NED operated by the Jet Propulsion Laboratory, California Institute of Technology, under contract with the National Aeronautics and Space Administration), of the NASA/ IPAC Infrared Science Archive (operated by the Jet Propulsion Laboratory, California Institute of Technology, under contract with the National Aeronautics and Space Administration) and of the LEDA database.

## References

- Balmaverde, B. & Capetti, A. 2006a, A&A in press, astro-ph/0601175
- Balmaverde, B. & Capetti, A. 2006b, A&A(Paper II), 447, 97
- Begelman, M. C., Blandford, R. D., & Rees, M. J. 1980, Nature, 287, 307
- Capetti, A. & Balmaverde, B. 2005, A&A, 440, 73 (Paper I)
- Capetti, A., Kleijn, G. V., & Chiaberge, M. 2005, A&A, 439, 935
- Chiaberge, M., Capetti, A., & Macchetto, F. D. 2005, ApJ, 625, 716
- Cirasuolo, M., Celotti, A., Magliocchetti, M., & Danese, L. 2003, MNRAS, 346, 447
- de Ruiter, H. R., Parma, P., Capetti, A., et al. 2005, A&A, 439, 487
- Dietrich, M., Hamann, F., Shields, J. C., et al. 2002, ApJ, 581, 912
- Dunlop, J. S., McLure, R. J., Kukula, M. J., et al. 2003, MNRAS, 340, 1095
- Faber, S. M., Tremaine, S., Ajhar, E. A., et al. 1997, AJ, 114, 1771
- Filho, M. E., Barthel, P. D., & Ho, L. C. 2002, ApJS, 142, 223
- Filho, M. E., Fraternali, F., Markoff, S., et al. 2004, A&A, 418, 429
- George, I. M., Mushotzky, R. F., Yaqoob, T., et al. 2001, ApJ, 559, 167
- Graham, A. W., Erwin, P., Trujillo, I., & Asensio Ramos, A. 2003, AJ, 125, 2951
- Ho, L. C., Filippenko, A. V., & Sargent, W. L. W. 1997, ApJS, 112, 315
- Ho, L. C. & Peng, C. Y. 2001, ApJ, 555, 650
- Huchra, J., Davis, M., Latham, D., & Tonry, J. 1983, ApJS, 52, 89
- Kellermann, K. I., Sramek, R. A., Schmidt, M., Green, R. F., & Shaffer, D. B. 1994, AJ, 108, 1163
- Khochfar, S. & Burkert, A. 2003, ApJ, 597, L117
- Kormendy, J. & Richstone, D. 1995, ARA&A, 33, 581
- Krajnović, D. & Jaffe, W. 2002, A&A, 390, 423
- Lauer, T. R., Faber, S. M., Gebhardt, K., et al. 2005, AJ, 129, 2138
- Ledlow, M. J., Owen, F. N., & Keel, W. C. 1998, ApJ, 495, 227
- Machacek, M. E., Jones, C., & Forman, W. R. 2004, ApJ, 610, 183
- Maia, M. A. G., Machado, R. S., & Willmer, C. N. A. 2003, AJ, 126, 1750
- Makino, J. & Funato, Y. 2004, ApJ, 602, 93
- Mannucci, F., Basile, F., Poggianti, B. M., et al. 2001, MNRAS, 326, 745
- Marconi, A. & Hunt, L. K. 2003, ApJ, 589, L21
- Milosavljević, M., Merritt, D., Rest, A., & van den Bosch, F. C. 2002, MNRAS, 331, L51
- Nagar, N. M., Falcke, H., Wilson, A. S., & Ho, L. C. 2000, ApJ, 542, 186
- Nagar, N. M., Falcke, H., Wilson, A. S., & Ulvestad, J. S. 2002, A&A, 392, 53
- Nagar, N. M., Wilson, A. S., Mulchaey, J. S., & Gallimore, J. F. 1999, ApJS, 120, 209
- Narayan, R. 2004, ArXiv Astrophysics e-prints
- Narayan, R. & Yi, I. 1995, ApJ, 444, 231
- Netzer, H., Chelouche, D., George, I. M., et al. 2002, ApJ, 571, 256
- Pellegrini, S. 2005, ApJ, 624, 155
- Ravindranath, S., Ho, L. C., & Filippenko, A. V. 2002, ApJ, 566, 801
- Ryden, B. S., Forbes, D. A., & Terlevich, A. I. 2001, MNRAS, 326, 1141
- Sadler, E. M., Jenkins, C. R., & Kotanyi, C. G. 1989, MNRAS, 240, 591
- Seigar, M., Carollo, C. M., Stiavelli, M., de Zeeuw, P. T., & Dejonghe, H. 2002, AJ, 123, 184
- Sérsic, J.-L. 1968, Atlas de Galaxias Australes(Córdoba: Obs. Astron.)
- Slee, O. B., Sadler, E. M., Reynolds, J. E., & Ekers, R. D. 1994, MNRAS, 269, 928
- Terashima, Y. & Wilson, A. S. 2003, ApJ, 583, 145
- Tremaine, S., Gebhardt, K., Bender, R., et al. 2002, ApJ, 574, 740

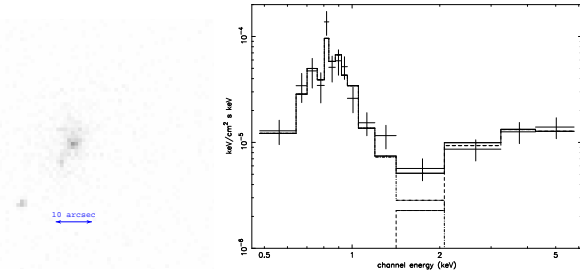


**Fig. A.1.** Chandra image and spectrum for UGC 7103. The fit and the contributions of the two components (thermal and power-law) are also plotted.

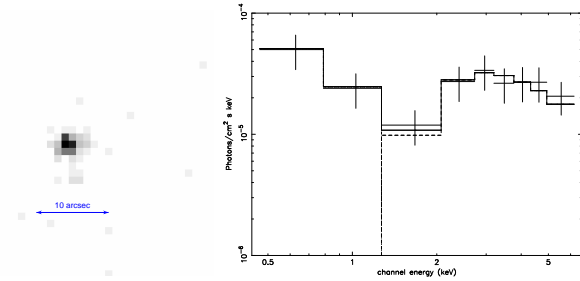


**Fig. A.2.** Chandra image and spectrum for UGC 8675. The fit and the contributions of the two components (thermal and power-law) are also plotted.

Wilson, A. S. & Colbert, E. J. M. 1995, ApJ, 438, 62

Wrobel, J. M. 1991, AJ, 101, 127

Wrobel, J. M. & Heeschen, D. S. 1991, AJ, 101, 148

## Appendix A: Notes on the X-ray observations of the individual sources

In this Appendix we list references and provide comments for the Chandra data and X-ray nuclear measurements found in the literature.

We also summarise of the results of the data analysis for the unpublished Chandra observations for 3 galaxies in Table A.1. We analysed these observations following the same strategy as in Balmaverde & Capetti (2006b). Briefly, using the Chandra data analysis CIAO v3.0.2, with the CALDB version 2.25, we reprocessed all the data from level 1 to level 2, subtracting the bad pixels, applying ACIS CTI correction, coordinates, and pha randomization. We searched for background flares and eventually we excluded some period of bad aspect. We extracted the spectrum in a circle region centred on the nucleus with radius of  $2''$ , measuring the background in an annulus of  $4''$  radius. We then fit the spectrum using an absorbed power-law plus a thermal model, with the hydrogen column density fixed at the Galactic value. In Figs. A.1 and A.2 we give images and spectra for the 2 newly detected X-ray nuclei.

**UGC 5617:** The spectrum of the nuclear source is fitted with an absorbed power-law with a photon index  $\Gamma = 1.94^{+0.26}_{-0.25}$  and an intrinsic absorption of  $N_H = 4.8 \cdot 10^{21} \text{cm}^{-2}$  George et al. (2001).

**UGC 5663:** Filho et al. (2004) find a hard nuclear X-ray source, spatially coincident with the optical nucleus. The spectrum of the nuclear source is fitted with a power-law ( $\Gamma$  fixed at value 1.7).

**UGC 6153:** Netzer et al. (2002) fitted the spectrum obtained with the Chandra Low Energy Transmission Grating using a photon index  $\Gamma=1.7$  plus a reflection spectrum of gas with a column density of  $N_H=10^{24} \text{cm}^{-2}$  and a covering factor of 0.4-0.7.

**UGC 7103:** We fitted the spectrum with an absorbed powerlaw ( $N_H = 4.6 \cdot 10^{22} \text{cm}^{-2}$  and a photon index  $\Gamma$  fixed to 1.9) plus a thermal model.

**UGC 7142:** In a circle of radius  $2''$  Terashima & Wilson (2003) obtained total nuclear counts of 32.6 in the 2-8 keV range. A power-law model modified by absorption was applied to the data obtaining  $\Gamma = 1.66$  and  $N_H = 1.5 \cdot 10^{20} \text{cm}^{-2}$ .

**UGC 7256:** Ho & Peng (2001) measured 410 nuclear counts from a  $2''$  diameter circle. The ACIS count rate are converted to x-ray luminosity by assuming  $\Gamma = 1.8$  and  $N_H = 2 \cdot 10^{20} \text{cm}^{-2}$ .

**UGC 7575:** Machacek et al. (2004) analysed the total emission from the galaxy (within  $32''$  of the nucleus). The data were described by a thermal MEKAL plasma plus a power-law component. Fixing the absorbing column at the Galactic value ( $2.64 \cdot 10^{22} \text{cm}^{-2}$ ) and the MEKAL model abundance at  $0.1 Z_\odot$ , the data are well fitted with a photon index  $\Gamma = 1.22$ .

**UGC 7614:** We estimated an upper limit to any non-thermic emission fixing the photon index to  $\Gamma=1.9$ .

**UGC 8675:** We grouped the data to have at least 10 counts per channel and we applied the Poissonian statistic. The spectrum is fitted using an absorbed powerlaw ( $N_H = 4.4 \cdot 10^{22} \text{cm}^{-2}$  and photon index  $\Gamma$  fixed to 1.9) plus a thermal model.

**Table A.1.** Summary of the results of the data analysis for the 3 unpublished Chandra observations

| Name     | Observation information |            |        |          | Fit results             |             |                     |                            |                                   |
|----------|-------------------------|------------|--------|----------|-------------------------|-------------|---------------------|----------------------------|-----------------------------------|
|          | Obs Id                  | date       | Inst   | Exp time | $N_H^z$                 | $\Gamma$    | KT                  | $F_{x,nuc}(1 \text{ keV})$ | $\chi^2/\text{d.o.f}$ or PHA bins |
| UGC 7103 | 1578                    | 2001-04-03 | ACIS-S | 15.0     | $4.6_{-1.8}^{+3.2}$ E22 | 1.9 (fixed) | $0.6_{-0.1}^{+0.1}$ | $1.0_{-0.3}^{+0.4} E - 13$ | 7.3/15                            |
| UGC 7614 | 2927                    | 2002-06-02 | ACIS-S | 10.0     | –                       | 1.9 (fixed) | –                   | $< 1.9 E - 14$             | –                                 |
| UGC 8675 | 415                     | 2000-09-03 | ACIS-S | 2.0      | $4.4_{-1.1}^{+1.4}$ E22 | 1.9 (fixed) | $0.4_{-0.1}^{+0.3}$ | $8.2_{-1.8}^{+3.3} E - 13$ | 9 PHA bins                        |